Bioorganic & Medicinal Chemistry 23 (2015) 4638–4648

Contents lists available at ScienceDirect

Bioorganic & Medicinal Chemistry

journal homepage: www.elsevier.com/locate/bmc

Discovery of an 8-methoxytetrahydroisoquinoline derivative as an orally active N-type calcium channel blocker for neuropathic pain without CYP inhibition liability

Takashi Ogiyama [a,*], Koichi Yonezawa [a], Makoto Inoue [a], Naoko Katayama [a], Toshihiro Watanabe [a], Seiji Yoshimura [a], Takayasu Gotoh [a], Tetsuo Kiso [a], Akiko Koakutsu [b], Shuichiro Kakimoto [a], Jun-ichi Shishikura [a]

[a] Drug Discovery Research, Astellas Pharma Inc., 21 Miyukigaoka, Tsukuba, Ibaraki 305-8585, Japan
[b] Drug Discovery Research, Astellas Pharma Inc., 2-1-6 Kashima, Yodogawa-ku, Osaka 532-8514, Japan

ARTICLE INFO

Article history:
Received 20 April 2015
Revised 28 May 2015
Accepted 29 May 2015
Available online 3 June 2015

Keywords:
N-type calcium channel
CaV2.2
Pain
CYP2D6
CYP3A4

ABSTRACT

In lead optimization efforts starting from the tetrahydroisoquinoline (*S*)-**1**, we identified 2-{[(2*R*)-2-hydroxypropyl]amino}-1-[(1*S*)-8-methoxy-1-phenyl-3,4-dihydroisoquinolin-2(1*H*)-yl]ethanone ((1*S*)-**8t**) as a novel orally active small-molecule N-type calcium channel blocker without CYP inhibition liability. CYP3A4 inhibition profile was improved by reducing the lipophilicity of compound (*S*)-**1**. Moreover, introduction of a methoxy group to the C-8 position of tetrahydroisoquinoline led to identification of (1*S*)-**8t**, which eliminated CYP2D6 inhibition liability. Oral administration of (1*S*)-**8t** exerted efficacy in a rat spinal nerve ligation (SNL) model of neuropathic pain with an ED_{50} value of 2.8 mg/kg.

1. Introduction

N-type (Cav2.2) calcium channels are primarily localized at presynaptic terminals in afferent Aδ- or C-fiber endings of lamina I and II, and play a prominent role in controlling the transmission of nociceptive information. Numerous lines of evidence have proved that N-type calcium channels are profoundly involved in the pain pathway.[1] The marketed peptide drug ziconotide exhibits clinical efficacy in the treatment of chronic pain via the blockade of N-type calcium channels. However, the clinical utility of ziconotide is limited by its requirement for intrathecal administration and severe CNS adverse effects.[2] Therefore, recent studies have focused on identifying small-molecule N-type calcium channel blockers which overcome these drawbacks.[3,4]

We previously identified 1-isopropyltetrahydroisoquinoline (*R*)-**2** as a potent N-type calcium channel blocker for the treatment of neuropathic pain in lead optimization efforts from 1-cyclohexyltetrahydroisoquinoline (*S*)-**1** (Table 1).[5a] Oral administration of (*R*)-**2** improved mechanical allodynia in a rat spinal nerve ligation (SNL) model of neuropathic pain with an ED_{50} value of 2.5 mg/kg. Unlike the case with ziconotide, no abnormal behavior was observed in test animals. In addition, reducing the lipophilicity of compound (*S*)-**1** by replacing the 1-cyclohexyl group with a 1-isopropyl moiety led to the elimination of CYP3A4 inhibition liability while maintaining N-type calcium channel inhibitory potency ((*S*)-**1** versus (*R*)-**2**).

Human cytochrome P450 (CYP) enzymes are membrane-associated proteins which contain heme as a prosthetic group. These enzymes are found in the inner membrane of the mitochondria and endoplasmic reticulum of cells. Some isoforms of these enzymes (i.e. CYP1A2, 2D6, 2C9, 2C19, and 3A4) play a crucial role in the metabolic elimination of drugs. CYP2D6 participates in the metabolism of about 25% of clinically available drugs, although hepatic abundance of CYP2D6 is less than 5% of all CYP enzymes.[6] Inhibition of CYP2D6 occasionally causes unwanted drug-drug interactions (DDIs), as shown by combination of the selective serotonin reuptake inhibitors (SSRIs) fluoxetine and paroxetine, which are potent CYP2D6 inhibitors, and tricyclic antidepressants (TCAs), which are metabolized by CYP2D6.[6] To mitigate risks in drug development and maximize convenience in clinical use, drug discovery efforts should focus on minimizing issues related to CYP2D6-mediated DDIs.

In an attempt to eliminate CYP2D6 inhibition liability while maintaining potency for N-type calcium channel inhibition,

* Corresponding author. Tel.: +81 29 863 6683; fax: +81 29 852 5387.
E-mail address: takashi.ogiyama@astellas.com (T. Ogiyama).

http://dx.doi.org/10.1016/j.bmc.2015.05.053
0968-0896/

Table 1
In vitro pharmacological properties of (*S*)-**1** and (*R*)-**2**

Compound	N-type FLIPR IC_{50} (μM)	CYP2D6 IC_{50} (μM)	CYP3A4[a] Preincubation time		*c*log$D_{7.4}$[b]
			0 min	30 min	
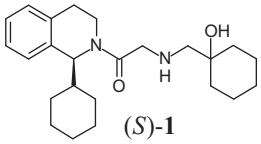 (*S*)-**1**	1.0	0.60	87%	67%	3.48
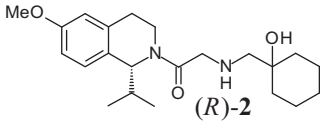 (*R*)-**2**	1.9	2.9	99%	92%	2.55

[a] Residual activities (%) of HLM were evaluated using midazolam as a probe substrate. Details are described in the experimental section.
[b] *c*log*D* values at pH 7.4 were calculated with ACD/PhysChem Batch (version 12.01).

introduction of various substituents on the phenyl ring of 1-isopropyl tetrahydroisoquinoline was examined.[5] Through this effort, we identified 6-methoxy derivative (*R*)-**2**. The inhibitory activity of (*R*)-**2** against CYP2D6 was approximately 5-fold weaker than that of lead compound (*S*)-**1** ((*S*)-**1** versus (*R*)-**2**) however, (*R*)-**2** still exhibited moderate potency for CYP2D6 inhibition. Further optimization of reducing CYP2D6 inhibition liability starting from 1-isopropyl tetrahydroisoquinoline (*R*)-**2** therefore appeared difficult. In addition, the previous results raised the possibility that conformational alterations might help to reduce CYP2D6 inhibition liability, particularly those induced by steric repulsion of two bulky substituents between the C-1 and C-8 positions of tetrahydroisoquinoline.[5b]

We therefore pursued a second approach to lead optimization starting from (*S*)-**1**. Here, we describe the design and synthesis of a novel series of tetrahydroisoquinolines, and the discovery of (1*S*)-**8t** as an orally active small-molecule N-type calcium channel blocker with the elimination of CYP inhibition liability.

2. Chemistry

Synthesis of tetrahydroisoquinoline derivatives **5**–**11** is illustrated in Scheme 1. Tetrahydroisoquinoline derivatives (**5**–**7**, **8a**–**8e**, and **9**–**11**) were prepared by substitution of the chloroacetamide **3a**–**3e** with amines. (1*S*)-**8a** was synthesized from (1*S*)-**3a**[5a,13] with (2*R*)-1-amino-2-propanol. Tetrahydroisoquinoline derivatives (**8f**–**8p**, (1*S*)-**8q**, **8r**, **8s**, (1*S*)-**8t**, and (1*R*)-**8t**) were synthesized from the tetrahydroisoquinolines (**4f**–**4p**, (1*S*)-**4q**, **4r**, **4s**, (1*S*)-**4t**, and (1*R*)-**4t**) in a two-step sequence. Compound (1*S*)-**8q** was synthesized from (1*S*)-**4q**, which was obtained from a commercial source. Absolute configuration of (1*S*)-**4t** was confirmed by vibrational circular dichroism (VCD) spectrum analysis of its synthetic intermediate (1*S*)-5-bromo-8-methoxy-1-phenyl-1,2,3,4-tetrahydroisoquinoline ((1*S*)-**22**).[7] Preparations of the chloroacetamides (**3b**–**3e**) and tetrahydroisoquinolines (**4f**–**4p**, and **4r**, **4s**, (1*S*)-**4t**, and (1*R*)-**4t**) are described in Supporting information.

3. Results and discussion

Inhibitory activity against N-type calcium channels was evaluated using the fluorometric imaging plate reader (FLIPR) calcium imaging assay in IMR-32 human neuroblastoma cells. Experiments were conducted in the presence of nitrendipine to block endogenous L-type calcium channels. The nociceptive responses to chemical stimuli were evaluated in the second phase of the formalin test in mice. Selected compounds were assessed for inhibitory activity against CYP2D6 using a fluorescence substrate. The reversible and time-dependent inhibitory (TDI) effects of selected compounds were evaluated using midazolam as a probe substrate to monitor changes in CYP3A4 activity.

In keeping with the implications of the last investigation,[5] we conducted lead optimization from (*S*)-**1** while retaining the bulky 1-cyclohexyl moiety. It is well documented that lipophilic compounds tend to have CYP inhibition liability.[8b,9] In addition, reducing the lipophilicity of 1-substituted tetrahydroisoquinoline led to an improvement in CYP3A4 inhibition liability while retaining potency for N-type calcium channel inhibition in our investigation.[5b] To explore another approach to reducing the lipophilicity of (*S*)-**1**, we investigated the effect of transformation of a second hydrophobic cyclohexyl moiety which linked to a basic nitrogen through a glycine linker (Table 2). To reduce CYP3A4 liability, we designed compounds mainly reference to the *c*log$D_{7.4}$ value. To ensure efficient screening, we prepared and evaluated the diastereomixture of compounds except for (1*S*)-**8q** and **8t**. Drastic differences in in vitro pharmacological profiles between the diastereomixture and biologically active isomer were not observed, as exemplified by **8a** and (1*S*)-**8a** (Table 2).

Replacement of cyclohexyl moiety in compound **1** with dimethyl group (**5**) resulted in an approximately 2-fold decrease in N-type calcium channel blockade. Transformation to hydroxybutylamine (**6** and **7**) and hydroxypropylamine (**8a** and **9**) led to 2- to 2.5-fold decreases in potency for N-type calcium channel inhibition compared with compound **1**. The hydrophobic analog **10** showed an equivalent effect on N-type calcium channel inhibition compared with the hydrophilic analogs **6** and **9**. Another hydrophobic analog **11** showed a slight decrease in potency for N-type calcium channels compared with compound **1**. Taken together, these results demonstrated that there is no correlation between inhibitory activity against N-type calcium channels and the lipophilicity of this part. Compound **5** lacked an antinociceptive effect in the formalin test in mice. Compounds **6** and **7** both showed only weak antinociceptive activity. Compound **8a** showed an adequate antinociceptive effect, although compound **9** did not produce any antinociceptive effect. The antinociceptive activity of compound **10** was comparable to that of compound **8a**. Compound **11** showed slightly weak antinociceptive activity compared with compound **8a** and **10**. Regarding CYP2D6 inhibition liability, the relationship with the lipophilicity of the compound was obscure as well as our previous study.[5b] Transformations into hydrophilic groups (**6**, **8a**, and **9**) afforded small

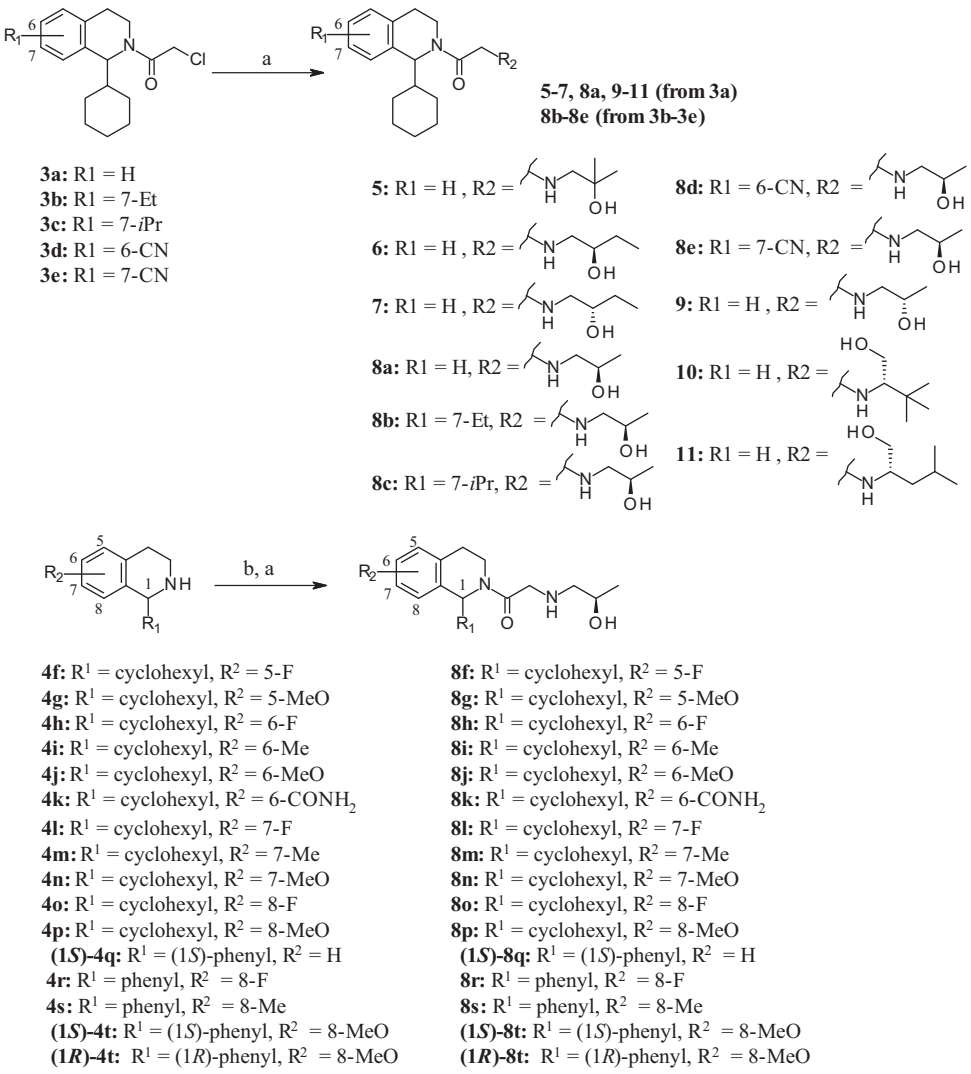

Scheme 1. Reagents and conditions: (a) amine, K_2CO_3, MeCN, 60 °C, 3 h; (b) chloroacetyl chloride, sat. $NaHCO_3$ aq, AcOEt, rt, 1 h.

improvements in CYP2D6 liability compared with compound **1**. Highly hydrophobic compounds **10** and **11** were potent CYP2D6 inhibitors. In contrast, CYP3A4 inhibition liability correlated with the lipophilicity of a compound to some extent. The less lipophilic compounds **6** and **7** ($c\log D_{7.4}$ = 2.60) showed an improvement in the TDI liability of CYP3A4 compared with compound **1** ($c\log D_{7.4}$ = 3.48). The much less lipophilic analogs **8a** and **9** ($c\log D_{7.4}$ = 2.53) exhibited favorable CYP3A4 inhibition profiles compared with compounds **6** and **7** ($c\log D_{7.4}$ = 2.60). Hydrophobic compounds **10** and **11**, whose log $D_{7.4}$ value were around 3.8, showed marked deterioration in CYP3A4 inhibition profiles compared with compound **1**. Overall, compound **8a**, which has a (2*R*)-hydroxypropylamine group, exhibited a favorable profile. In addition, the biologically active isomer (1*S*)-**8a** exhibited desirable in vivo efficacy compared with diastereomixture of **8a**, although the other in vitro profiles of (1*S*)-**8a** are almost equivalent to those of **8a**. de Groot et al. provided knowledge-based general strategies to address CYP2D6 inhibition liability.[9b] According to their suggestion, small modifications to the periphery of the molecule, such as the exchange of substituents on the benzene moiety, could have a significant impact on reducing CYP2D6 inhibition liability. Thus, we next investigated the effect of substituents on the benzene ring in tetrahydroisoquinoline of compound **8a** to address CYP2D6 inhibition liability (Table 3).

5-Fluorine substituted analog **8f** exhibited favorable potency for N-type calcium channel inhibition. Introduction of the 5-methoxy (**8g**) to compound **8a** did not affect the enhancement of potency for N-type calcium channel inhibition. Both compounds **8f** and **8g** resulted in deterioration in the TDI profile of CYP3A4. Among compounds substituted at the C-6 position of tetrahydroisoquinoline (**8h**, **8i**, **8j**, **8d**, and **8k**), compound **8h** (R = 6-F) showed relatively favorable inhibitory activity against N-type calcium channels. Introduction of hydrophilic 6-substituents, such as cyano (**8d**) and carbamoyl (**8k**) groups, resulted in a decrease or complete loss of potency for N-type calcium channels. Compound **8h** (R = 6-F) and **8j** (R = 6-MeO) showed favorable CYP3A4 inhibition liability as well as compound **8a**. Incorporation of substituents (**8l**, **8m**, **8b**, **8c**, **8n**, and **8e**) into tetrahydroisoquinoline at the C-7 position resulted in relatively preferable N-type calcium channel inhibition, except for the fluorine (**8l**) and cyano (**8e**) groups. In particular, compound **8b** (R = 7-ethyl) showed optimal potency in this study. However, 7-substituted compounds (**8b**, **8c**, **8l**, and **8n**), particularly the lipophilic alkyl substituted analogs of **8b** and **8c**, showed a deterioration of TDI profile of CYP3A4 compared with compound **8a** ($c\log D_{7.4}$ = 3.63, 3.29 vs 2.53). Inhibitory activity of compound **8p** (R = 8-methoxy) against N-type calcium channels was more favorable than that of compound **8o** (R = 8-fluorine). Regarding potency for N-type calcium channel inhibition, apparent

Table 2
Effect of 1-cyclohexyltetrahydroisoquinoline derivatives on N-type calcium channel potency, CYP 2D6 and 3A4 inhibitory activities

Compound no.	N-type FLIPR IC_{50} (μM)	Formalin test % inhibition[a]	CYP2D6 IC_{50} (μM)	CYP3A4[b] Preincubation time 0 min	CYP3A4[b] Preincubation time 30 min	$c\log D_{7.4}$[c]
1	0.77	62	0.78	86%	61%	3.48
5	1.7	7.7	N.T.	N.T.	N.T.	2.94
6	1.5	19	1.0	87%	88%	2.60
7	1.9	27	<0.3	81%	83%	2.60
8a	2.0	39	1.1	92%	95%	2.53
9	1.5	0	1.6	96%	91%	2.53
10	1.4	40	0.068	65%	33%	3.77
11	1.1	32	0.044	69%	46%	3.80
(1*S*)-**8a**	1.7	55	1.4	105%	87%	2.53

[a] At 100 mg/kg p.o.
[b] Residual activities (%) of HLM were evaluated using midazolam as a probe substrate. Details are described in the experimental section.
[c] *c*log*D* values at pH 7.4 were calculated with ACD/PhysChem Batch (version 12.01).

structure–activity relationships (SARs) were not observed. However, compounds which exhibited potent inhibitory activity against N-type calcium channels (IC_{50} <2 μM) tended to possess relatively high lipophilicity ($c\log D_{7.4}$ value >2.3 or more). Introduction of an 8-methoxy group (**8p**) led to a deterioration in CYP3A4 inhibition liability due to lipophilicity ($c\log D_{7.4}$ = 3.07). Regarding CYP2D6 inhibition liability, no apparent improvement was observed in evaluated compounds, except for compounds **8n** (R = 7-methoxy) and **8p** (R = 8-methoxy). Introduction of a 7-methoxy group (**8n**) only led to a greater than 3-fold attenuation of CYP2D6 inhibition compared with **8a**. Notably, introduction of an 8-methoxy group (**8p**) led to significant attenuation of CYP2D6 inhibition liability. The marked improvement in CYP2D6 inhibition liability was the first observation of our study.[5b]

In the course of the discovery of (*R*)-**2**, 1-phenyl (*S*)-**12**, which like 1-cyclohexyl (*S*)-**1** had a bulky substituent at the C-1 position of the tetrahydroisoquinoline, was synthesized and found to exhibit much less lipophilicity than (*S*)-**1** ($c\log D_{7.4}$ value (*S*)-**12**: 2.75 vs (*S*)-**1**: 3.48) with an equivalent in vitro profile to (*S*)-**1** (Table 4).[5b] Given our results so far, transformation of the 1-cyclohexyl group of **8p** to the 1-phenyl group could improve CYP3A4 profile with retention of favorable CYP2D6 inhibition liability due to its less lipophilic nature and bulkiness. Therefore, we investigated the effect on incorporation of substituents into the C-8 position of 1-phenyl tetrahydroisoquinoline (Table 5). As expected, compound (1*S*)-**8q** exhibited an almost equivalent in vitro profile to (1*S*)-**8a** with decreased lipophilicity ($c\log D_{7.4}$ value (1*S*)-**8q**: 1.80 vs (1*S*)-**8a**: 2.53). Introduction of a fluorine group (**8r**) showed preferable potency for N-type calcium channel inhibition in spite of an exceptionally low lipophilic property. Inhibitory activity of the methyl group (**8s**) and *S*-isomer of the methoxy group ((1*S*)-**8t**) exhibited comparable potency for N-type calcium channel inhibition to **8p** and was superior to that of *R*-isomer (1*R*)-**8t**. As expected, these compounds (**8r**, **8s**, (1*S*)-**8t** and (1*R*)-**8t**) exhibited desirable CYP3A4 inhibition profiles due to the weaker lipophilic properties than **8p** (log $D_{7.4}$ values: 1.33–2.35 vs 3.07). Regarding CYP2D6 inhibition, introduction of methyl group **8s** resulted in over 2-fold attenuation compared with compound (1*S*)-**8q**. Moreover, (1*S*)-**8t** completely eliminated CYP2D6 inhibition liability. These results are consistent with our expectation and indicated that the attenuation of CYP2D6 inhibition liability resulted from conformational changes, induced by steric repulsion between the 8-substituted group and 1-phenyl moiety of tetrahydroisoquinoline (1*S*)-**8t**.

Based on the X-ray crystal structure of human CYP2D6 bound with 10-{2-[(2*R*)-1-methylpiperidin-2-yl]ethyl}-2-(methylsulfanyl)-10*H*-phenothiazine (RTZ),[10] which is known as a non-heme binder, the interaction of (1*S*)-**8q** with CYP2D6 was examined to obtain a better understanding of why (1*S*)-**8t** led to a significant decrease in CYP2D6 inhibition liability. Molecular docking was performed between (1*S*)-**8q** and CYP2D6, on the assumption that the binding site of (1*S*)-**8q** was around RTZ, as indicated by their

Table 3
Inhibitory effect of tetrahydroisoquinoline substitutions on N-type calcium channels, CYP 2D6 and 3A4

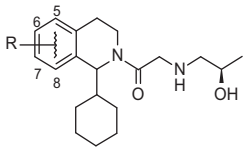

R (compound no.)	N-type FLIPR IC_{50} (μM)	CYP2D6 IC_{50} (μM)	CYP3A4[a] Preincubation time		$c\log D_{7.4}$[b]
			0 min	30 min	
H(**8a**)	2.0	1.1	92%	95%	2.53
5-F (**8f**)	1.2	<0.39	95%	49%	2.34
5-MeO (**8g**)	2.0	<0.78	107%	63%	3.08
6-F (**8h**)	1.6	1.6	92%	91%	2.71
6-Me (**8i**)	2.4	N.T.	N.T.	N.T.	2.96
6-MeO (**8j**)	1.9	<0.78	93%	97%	2.72
6-CN (**8d**)	3.1	N.T.	N.T.	N.T.	2.05
6-$CONH_2$ (**8k**)	>10	N.T.	N.T.	N.T.	1.31
7-F (**8l**)	2.3	1.3	109%	80%	2.39
7-Me (**8m**)	1.7	N.T.	N.T.	N.T.	3.12
7-Et (**8b**)	0.89	1.3	85%	65%	3.63
7-iPr (**8c**)	1.3	1.9	88%	43%	3.29
7-MeO (**8n**)	1.6	3.7	97%	83%	2.99
7-CN (**8e**)	2.6	N.T.	N.T.	N.T.	2.30
8-F (**8o**)	2.5	N.T.	N.T.	N.T.	2.05
8-MeO (**8p**)	1.4	30.2	85%	58%	3.07

[a] Residual activities (%) of HLM were evaluated using midazolam as a probe substrate. Details are described in the experimental section.
[b] *c*log*D* values at pH 7.4 were calculated with ACD/PhysChem Batch (version 12.01).

3D-pharmacophore resemblance. The binding modes of (1*S*)-**8q** and RTZ in the CYP2D6 crystal structure are illustrated in Fig. 1a. In this model, the two aromatic parts of (1*S*)-**8q** overlap with the phenothiazine ring of RTZ, and the basic part of both inhibitors are shown to interact with Asp^{301}, which is a key acidic residue which interacts with basic CYP2D6 inhibitors. Given that (1*S*)-**8q** interacts with CYP2D6 in a manner similar to RTZ, as the model strongly suggested, the potency of (1*S*)-**8q** for CYP2D6 inhibition (IC_{50} = 2.2 μM) could be explained by the following two reasons. First, three critical electrostatic interactions were observed in the model, namely hydrogen bonding between the hydroxypropyl group of (1*S*)-**8q** and a hydroxyl group in Ser^{304}, salt bridge between the amino group of (1*S*)-**8q** and a carboxylic acid residue of Asp^{301}, and hydrogen bonding (CH...O interaction) between the carbonyl group of (1*S*)-**8q** and an alpha proton of Asp^{301}. Second, the overall (1*S*)-**8q** molecule showed potential hydrophobic interactions interpreted as donor-π, π–π and van der Waals interactions with Phe^{120}, Leu^{121}, Leu^{213}, Glu^{216}, Leu^{248}, Ala^{300}, Asp^{301}, Ser^{304} and Phe^{483} of CYP2D6 (Fig. 1b).

Whereas the phenyl ring of the tetrahydroisoquinoline (1*S*)-**8q** was tightly stacked by Phe^{120}, Glu^{216} and Phe^{483}, a relatively large pocket was spread out flat within the same plane as the aromatic ring, which could accommodate various substituents on tetrahydroisoquinoline. These observations imply that incorporation of substituents has no or little effect on the impairment of interactions with CYP2D6, which might explain why our attempt using a knowledge-based approach did not work, except for introduction of the 8-methoxy group of **8t**.

Interestingly, the 1-phenyl group was packed into the flat pocket formed by Ser^{304} and Leu^{213}, where the pocket was relatively narrow in the vertical direction of the 1-phenyl ring, indicating that the relative arrangement between tetrahydroisoquinoline and the 1-phenyl group was critical for binding to CYP2D6. Dihedral angle of (1*S*)-**8q** between tetrahydroisoquinoline and the 1-phenyl group was 114.8° in this model.

In addition, the dihedral angle of 8-methoxytetrahydroisoqinoline between tetrahydroisoquinoline and the 1-phenyl group in the most stable conformation was significantly different from that of tetrahydroisoquinoline, depending on the presence or absence of the 8-methoxy moiety (145.8° vs 130.2°).[11] Based on these results, we speculate that introduction of an 8-methoxy group to (1*S*)-**8q** led to a change in the relative arrangement between tetrahydroisoquinoline and the 1-phenyl group by steric repulsion with the 1-phenyl group, and that (1*S*)-**8t** was probably unable to fit into the CYP2D6 enzyme and thus exhibited a significant decrease in activity against CYP2D6.

Several knowledge-based strategies, such as modifying the periphery of the molecule or reducing the overall lipophilicity of the compound, have been proposed to reduce CYP2D6 inhibition liability and many successful studies based on these strategies have been reported.[8,9] However, in cases where knowledge-based approaches do not work or are not suitable to striking a balance with bioactivity against the target molecule or ADMET, considerable effort is required, such as in our study due to the large and flexible nature of the CYP2D6 binding pocket. Despite having been wise after the event, our result indicated that molecular docking simulation could guide many aspects of drug design. At present, we still lack understanding of CYP2D6 inhibition. For example, only one study has described the X-ray crystal structure of human

Table 4
In vitro pharmacological properties of (*S*)-**1** and (*S*)-**12**

Compound	N-type FLIPR IC_{50} (μM)	CYP2D6 IC_{50} (μM)	CYP3A4[a] Preincubation time		$c\log D_{7.4}$[b]
			0 min	30 min	
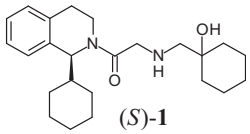 (*S*)-**1**	1.0	0.60	87%	67%	3.48
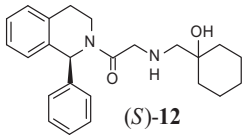 (*S*)-**12**	1.0	<0.39	89%	78%	2.75

[a] Residual activities (%) of HLM were evaluated using midazolam as a probe substrate. Details are described in the experimental section.
[b] *c*log*D* values at pH 7.4 were calculated with ACD/PhysChem Batch (version 12.01).

Table 5
Inhibitory activities on N-type calcium channels, CYP 2D6 and 3A4

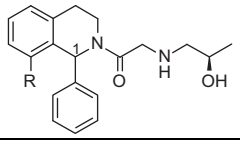

R (Compound No.)	N-type FLIPR IC_{50} (μM)	CYP2D6 IC_{50} (μM)	CYP3A4[a] Preincubation time		$clogD_{7.4}$[b]
			0 min	30 min	
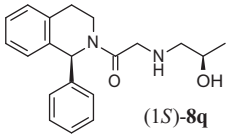 (1*S*)-**8q**	2.4	2.2	98%	94%	1.80
R = F (**8r**)	1.0	1.3	103%	95%	1.33
R = Me (**8s**)	1.3	5.6	100%	89%	2.14
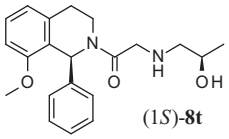 (1*S*)-**8t**	1.4	>50	94%	90%	2.35
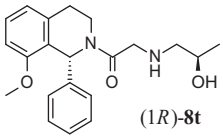 (1*R*)-**8t**	3.3	17.9	110%	91%	2.35

[a] Residual activities (%) of HLM were evaluated using midazolam as a probe substrate. Details are described in the experimental section.
[b] *c*log*D* values at pH 7.4 were calculated with ACD/PhysChem Batch (version 12.01).

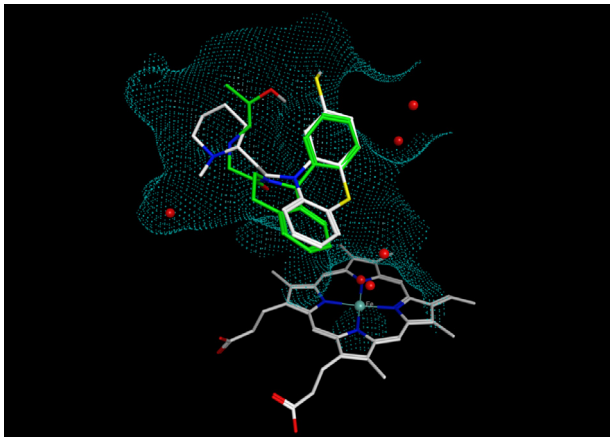

Figure 1a. Docking mode of (1*S*)-**8q** and crystal structure of RTZ in complex with human CYP2D6. Only the hetero molecules in the binding site are shown for clarity with the atoms colored as nitrogen—blue, oxygen—red, Fe—light blue, and carbon—white or green. The wall of the binding site is represented as a blue dotted surface and waters kept in the docking study are shown as red spheres. White carbon: RTZ and Heme in the crystal structure of human CYP2D6 (PDB ID: 3TBG). Green carbon: Docked conformation of (1*S*)-**8q**. (1*S*)-**8q** and RTZ occupied the same site, with aromatic and basic features in common position.

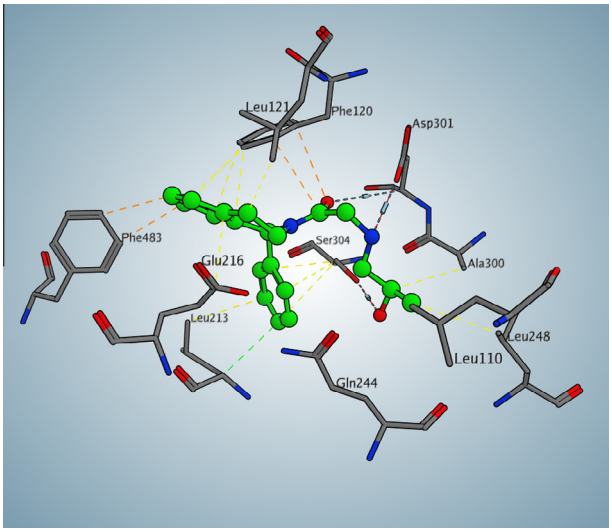

Figure 1b. Observed interactions in the docking model of (1*S*)-**8q** with the binding site residues of human CYP2D6. (1*S*)-**8q** is depicted as ball-and-stick model with the same color scheme as Figure 1a. Three hydrogen bonds (light blue rod) and many hydrophobic interactions (green: donor-π, orange: π–π, and yellow: van der Waals, indicated by Scorpion) are observed between (1*S*)-**8q** and CYP2D6, which support its potent inhibition of CYP2D6. Both Figure 1a and b were created using the Molecular Operating Environment (MOE 2013).

CYP2D6 bound with a non-heme binder. Given the large and flexible nature of CYP2D6, however, we speculate that several other sites able to bind with other CYP2D6 inhibitors are present. Use of structural information to attenuate CYP2D6 inhibition liability in the drug discovery process requires more information of the X-ray crystal structure of CYP2D6 bound with non-heme binders, and considerable additional investigation is accordingly needed.[8,9]

Encouraged by the result, further characterizations of compound (1*S*)-**8t** were conducted (Table 6). Regarding inhibitory activities against the three other major CYP450 isoforms (CYP1A2, 2C9 and 2C19), compound (1*S*)-**8t** exhibited no inhibitory activities. Moreover, compound (1*S*)-**8t** showed weak inhibitory activities against both L-type calcium channels (IC_{50} >10 μM) and hERG potassium channels (IC_{50} >100 μM). The human liver microsomal (HLM) stability of compound (1*S*)-**8t** (CL 45.9 mL/min/kg) exhibited approximately 5-fold better metabolic stability than compound (*S*)-**1** (CL 223.4 mL/min/kg). Together, these results prompted us to investigate its in vivo efficacy.

Table 6
Inhibitory activities of (1*S*)-**8t** against CYP isoforms, hERG and L-type calcium channel

Compound	CYP1A2 IC_{50} (μM)	CYP2C9 IC_{50} (μM)	CYP2C19 IC_{50} (μM)	hERG IC_{50} (μM)	L-type FLIPR IC_{50} (μM)
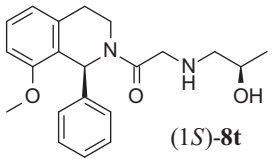 (1*S*)-**8t**	>50	>50	>50	>100	>10

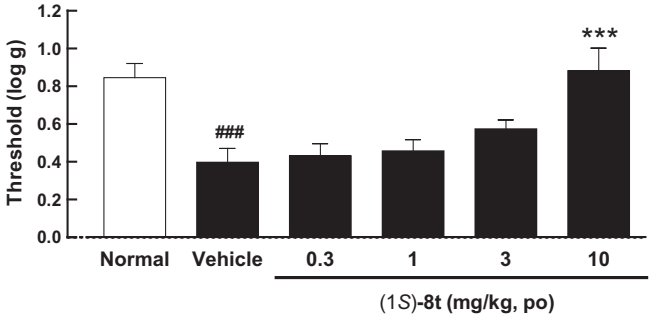

Figure 2. Effect of compound (1*S*)-**8t** on mechanical allodynia in SNL model rats. Each bar represents the mean ± SEM withdrawal threshold of the hindpaw ($n = 8$). ###$P < 0.001$, statistically significant compared with normal group (Student's *t*-test). ***$P < 0.001$, statistically significant compared with the vehicle-treated group (Dunnett's test). Closed columns, operated side paw in the drug-treated and vehicle-treated group. Open column, non-operated side paw in the vehicle-treated group.

Orally administrated (1*S*)-**8t** exhibited antinociceptive activity (77% inhibition) in the second phase of the formalin test in mice at 100 mg/kg. Moreover, the analgesic effect of (1*S*)-**8t** was evaluated using the L5/L6 SNL model of neuropathic pain in rats.[12] (1*S*)-**8t** dose-dependently reduced mechanical allodynia with oral administration from 0.3 to 10 mg/kg. Oral administration of (1*S*)-**8t** improved mechanical allodynia in the rat SNL model with an ED_{50} value of 2.8 mg/kg (Fig. 2).

4. Conclusion

In lead optimization efforts from (*S*)-**1**, we identified (1*S*)-**8t** as a novel orally active small-molecule N-type calcium channel blocker without CYP inhibition liability. Based on the previous results, improvement in CYP3A4 inhibition profile was achieved by reducing the lipophilicity of (*S*)-**1**. Incorporation of a methoxy group into the C-8 position of tetrahydroisoquinoline ((1*S*)-**8t**) resulted in the loss of potency for CYP2D6 inhibition (IC_{50} >50 μM). A docking study suggested that a change in the relative arrangement between tetrahydroisoquinoline and the 1-phenyl group by installation of 8-MeO group disfavored binding to CYP2D6 enzyme. Oral administration of (1*S*)-**8t** exhibited efficacy in the rat SNL model of neuropathic pain, with an ED_{50} value of 2.8 mg/kg.

5. Experimental section

5.1. Chemistry

5.1.1. General

All reactions were carried out using commercially available reagents and solvents without further purification. Column chromatography was performed using a Shoko Scientific SI series silica gel cartridge on Shoko Scientific Purif-α2. ^{1}H NMR spectra were recorded on a JNM-EX400 spectrometer. Chemical shifts are expressed in δ units (ppm) using tetramethylsilane as an internal standard. Abbreviations used for the signal patterns are as follows: s, singlet; d, doublet; t, triplet; q, quartet; sep., septet; m, multiplet; and br, broad. Mass spectra were recorded on a JEOL LX-2000 or Waters ZQ-2000 mass spectrometer. Elemental analysis was conducted using a Yanaco MT-5 microanalyzer. HPLC analysis was performed using a Daicel OD-H or AD-RH chiral column on a Hitachi HPLC system (L-7000 series) equipped with a UV source (210 or 230 nm). Specific rotations were measured using a HORIBA SEPA-300 polarimeter.

5.1.2. 1-(1-Cyclohexyl-3,4-dihydroisoquinolin-2(1*H*)-yl)-2-[(2-hydroxy-2-methylpropyl)amino]ethanone fumarate (5)

To a solution of compound **3a** (200 mg) in acetonitrile (3 mL) was added potassium carbonate (474 mg) and 1-amino-2-methyl-2-propanol (244 mg). The reaction mixture was stirred for 3 hours at 60 °C. The mixture was diluted with chloroform and water, filtered through a phase separation filter and the filtrate was concentrated in vacuo. The residue was purified by silica gel column chromatography, and eluted with chloroform-methanol to give the desired product as a colorless gum (198 mg). The gum was dissolved in 2-propanol (2 mL), and fumaric acid (67 mg) was added to the solution. The mixture was stirred at room temperature for 3 hours. The precipitate was filtered off to obtain the title compound **5** (185 mg, 59%) as a colorless solid. ^{1}H NMR (DMSO-d_6): This compound exists as a pair of rotamers at room temperature. δ 7.09–7.24 (4H, m), 7.11 (fumaric acid 2H, s), 7.13 (major isomer 1H, d, $J = 9.2$ Hz), 4.43 (minor isomer 1H, d, $J = 9.4$ Hz), 4.16–4.27 (minor isomer 1H, m), 3.59–3.69 (2H, m), 3.48–3.57 (1H, m), 3.22–3.32 (minor isomer 1H, m), 2.78–2.98 (2H, m), 1.46–1.78 (6H, m), 0.96–1.21 (11H, m); FAB MS *m*/*z*: 345 $[M+H]^+$.

5.1.3. 1-(1-Cyclohexyl-3,4-dihydroisoquinolin-2(1*H*)-yl)-2-{[(2*R*)-2-hydroxybutyl]amino}ethanone oxalate (6)

Compound **6** was synthesized using a similar protocol to that for compound **5**. Compound **6** was obtained in 50% yield as a colorless solid. ^{1}H NMR (DMSO-d_6): This compound exists as a pair of rotamers at room temperature. δ 7.13–7.26 (4H, m), 5.11 (1H, d, $J = 9.4$ Hz), 4.27–4.34 (minor isomer 1H, m), 3.51–4.26 (5H, m), 3.30–3.41 (minor isomer 1H, m), 2.72–3.03 (4H, m), 1.29–1.78 (7H, m), 0.96–1.22 (4H, m), 0.87 (3H, t, $J = 7.4$ Hz); FAB MS *m*/*z*: 345 $[M+H]^+$.

5.1.4. 1-(1-Cyclohexyl-3,4-dihydroisoquinolin-2(1*H*)-yl)-2-{[(2*S*)-2-hydroxybutyl]amino}ethanone oxalate (7)

Compound **7** was synthesized using a similar protocol to that for compound **5**. Compound **7** was obtained in 44% yield as a colorless solid. ^{1}H NMR (DMSO-d_6): This compound exists as a pair of rotamers at room temperature. δ 7.08–7.28 (4H, m), 7.11 (1H, d, $J = 9.3$ Hz), 4.28–4.35 (minor isomer 1H, m), 4.09–4.25 (1H, m), 3.96–4.07 (1H, m), 3.52–3.76 (3H, m), 3.28–3.39 (1H, m), 2.70–3.05 (4H, m), 1.28–1.79 (7H, m), 0.95–1.22 (4H, m), 0.86 (3H, t, $J = 7.4$ Hz); FAB MS *m*/*z*: 345 $[M+H]^+$.

5.1.5. 1-(1-Cyclohexyl-3,4-dihydroisoquinolin-2(1*H*)-yl)-2-{[(2*R*)-2-hydroxypropyl]amino}ethanone oxalate (8a)

Compound **8a** was synthesized using a similar protocol to that for compound **5**. Compound **8a** was obtained in 68% yield as a colorless solid. ^{1}H NMR (DMSO-d_6): This compound exists as a pair of rotamers at room temperature. δ 7.10–7.26 (4H, m), 5.01 (1H, d, J = 9.4 Hz), 4.28–4.34 (minor isomer 1H, m), 3.23–4.24 (5H, m), 2.69–3.04 (4H, m), 1.45–1.79 (6H, m), 0.93–1.27 (8H, m); FAB MS m/z: 331 $[M+H]^+$. Anal. Calcd for $C_{20}H_{30}N_2O_2{\cdot}C_2H_2O_4.0.8H_2O$: C, 60.76; H, 7.79; N, 6.44. Found: C, 60.73; H, 7.56; N, 6.41.

5.1.6. 1-[(1*S*)-1-Cyclohexyl-3,4-dihydroisoquinolin-2(1*H*)-yl]-2-{[(2*R*)-2-hydroxypropyl]amino}ethanone fumarate ((1*S*)-8a)

Compound (1*S*)-**8a** was synthesized using a similar protocol to that for compound **8a**, except that (1*S*)-cyclohexyl-1,2,3,4-tetrahydroisoquinoline[13] was used as a starting material. Compound (1*S*)-**8a** was obtained in 37% yield as a colorless solid. ^{1}H NMR (DMSO-d_6): δ 7.07–7.25 (4H, m), 6.53 (fumaric acid 2H, s), 5.12 (1H, d, J = 9.3 Hz), 2.29–3.93 (9H, m), 1.42–1.78 (6H, m), 0.89–1.29 (8H, m); FAB MS m/z: 331 $[M+H]^+$. Anal. Calcd for $C_{20}H_{30}N_2O_2{\cdot}C_4H_4O_4.0.1H_2O$: C, 64.29; H, 7.69; N, 6.25. Found: C, 64.24; H, 7.69; N, 6.21. $[\alpha]_D^{20}$ −30.7° (c = 0.1, MeOH).

5.1.7. 1-(1-Cyclohexyl-7-ethyl-3,4-dihydroisoquinolin-2(1*H*)-yl)-2-{[(2*R*)-2-hydroxypropyl]amino}ethanone oxalate (8b)

Compound **8b** was synthesized using a similar protocol to that for compound **5**. Compound **8b** was obtained in 67% yield as a colorless solid. ^{1}H NMR (DMSO-d_6): This compound exists as a pair of rotamers at room temperature. δ 7.17 (1H, d, J = 7.8 Hz), 7.03–7.09 (1H, m), 6.97 (1H, m), 5.07 (major isomer 1H, d, J = 9.4 Hz), 4.25–4.31 (minor isomer 1H, m), 4.09–4.22 (1H, m), 3.91–4.05 (2H, m), 3.61–3.70 (major isomer 1H, m), 3.50–3.60 (major isomer 1H, m), 3.28–3.37 (minor isomer 1H, m), 2.70–2.99 (4H, m), 2.51–2.61 (2H, m), 1.48–1.78 (6H, m), 0.95–1.21 (11H, m); ESI MS m/z: 359 $[M+H]^+$.

5.1.8. 1-(1-Cyclohexyl-7-isopropyl-3,4-dihydroisoquinolin-2(1*H*)-yl)-2-{[(2*R*)-2-hydroxypropyl]amino}ethanone oxalate (8c)

Compound **8c** was synthesized using a similar protocol to that for compound **5**. Compound **8c** was obtained in 69% yield as a colorless solid. ^{1}H NMR (DMSO-d_6): This compound exists as a pair of rotamers at room temperature. δ 7.06–7.15 (2H, m), 6.96–7.02 (1H, m), 5.07 (1H, d, J = 9.5 Hz), 3.89–4.33 (4H, m), 3.48–3.70 (2H, m), 3.26–3.38 (minor isomer 1H, m), 2.69–2.99 (6H, m), 1.47–1.81 (8H, m), 0.95–1.23 (18H, m); FAB MS m/z: 373 $[M+H]^+$.

5.1.9. 1-Cyclohexyl-2-{*N*-[(2*R*)-2-hydroxypropyl]glycyl}-1,2,3,4-tetrahydroisoquinoline-6-carbonitrile oxalate (8d)

Compound **8d** was synthesized using a similar protocol to that for compound **5**. Compound **8d** was obtained in 56% yield as a colorless solid. ^{1}H NMR (DMSO-d_6): This compound exists as a pair of rotamers at room temperature. δ 7.74 (1H, br s), 7.61–7.71 (1H, m), 7.36–7.44 (1H, m), 5.22 (major isomer 1H, d, J = 9.2 Hz), 4.44–4.53 (minor isomer 1H, m), 4.20–4.30 (minor isomer 1H, m), 4.16 (major isomer 1H, d, J = 16.2 Hz), 3.90–4.09 (2H, m), 3.56–3.73 (major isomer 2H, m), 3.29–3.38 (minor isomer 1H, m), 2.86–3.07 (3H, m), 2.69–2.82 (1H, m), 1.38–1.78 (6H, m), 0.89–1.25 (8H, m); FAB MS m/z: 356 $[M+H]^+$.

5.1.10. 1-Cyclohexyl-2-{*N*-[(2*R*)-2-hydroxypropyl]glycyl}-1,2,3,4-tetrahydroisoquinoline-7-carbonitrile oxalate (8e)

Compound **8e** was synthesized using a similar protocol to that for compound **5**. Compound **8e** was obtained in 60% yield as a colorless solid. ^{1}H NMR (DMSO-d_6): This compound exists as a pair of rotamers at room temperature. δ 7.66–7.75 (2H, m), 7.63 (minor isomer 1H, br s), 7.38–7.48 (1H, m), 5.20 (major isomer 1H, d, J = 9.4 Hz), 4.40–4.48 (minor isomer 1H, m), 4.20–4.29 (1H, m), 4.15 (major isomer 1H, d, J = 16.1 Hz), 3.90–4.09 (2H, m), 3.56–3.73 (major isomer 2H, m), 3.30–3.39 (minor isomer 1H, m), 3.07 (2H, t, J = 6.1 Hz), 2.85–3.00 (1H, m), 2.68–2.82 (1H, m), 1.37–1.79 (6H, m), 0.92–1.25 (8H, m); FAB MS m/z: 356 $[M+H]^+$.

5.1.11. 1-(1-Cyclohexyl-3,4-dihydroisoquinolin-2(1*H*)-yl)-2-{[(2*S*)-2-hydroxypropyl]amino}ethanone oxalate (9)

Compound **9** was synthesized using a similar protocol to that for compound **5**. Compound **9** was obtained in 66% yield as a colorless solid. ^{1}H NMR (DMSO-d_6): This compound exists as a pair of rotamers at room temperature. δ 7.09–7.27 (4H, m), 5.11 (major isomer 1H, d, J = 9.4 Hz) 3.25–4.36 (5H, m), 2.67–3.08 (4H, m), 1.45–1.78 (6H, m), 0.91–1.26 (8H, m); FAB MS m/z: 331 $[M+H]^+$.

5.1.12. 1-(1-Cyclohexyl-3,4-dihydroisoquinolin-2(1*H*)-yl)-2-{[(2*S*)-1-hydroxy-3,3-dimethylbutan-2-yl]amino}ethanone oxalate (10)

Compound **10** was synthesized using a similar protocol to that for compound **5**. Compound **10** was obtained in 68% yield as a colorless solid. ^{1}H NMR (DMSO-d_6): This compound exists as a pair of rotamers at room temperature. δ 7.09–7.26 (4H, m), 5.12 (major isomer 1H, d, J = 9.0 Hz), 3.53–4.45 (7H, m), 2.85–3.07 (2H, m), 1.45–1.79 (6H, m), 0.90–1.24 (14H, m); FAB MS m/z: 373 $[M+H]^+$.

5.1.13. 1-(1-Cyclohexyl-3,4-dihydroisoquinolin-2(1*H*)-yl)-2-{[(2*S*)-1-hydroxy-4-methylpentan-2-yl]amino}ethanone oxalate (11)

Compound **11** was synthesized using a similar protocol to that for compound **5**. Compound **11** was obtained in 68% yield as a colorless solid. ^{1}H NMR (DMSO-d_6): This compound exists as a pair of rotamers at room temperature. δ 7.10–7.26 (4H, m), 5.12 (major isomer 1H, dd, J = 1.6, 9.4 Hz), 4.41 (minor isomer 1H, d, J = 9.3 Hz), 2.79–4.31 (9H, m), 1.31–1.79 (9H, m), 0.95–1.26 (5H, m), 0.76–0.93 (6H, m); FAB MS m/z: 373 $[M+H]^+$.

5.1.14. 1-(1-Cyclohexyl-5-fluoro-3,4-dihydroisoquinolin-2(1*H*)-yl)-2-{[(2*R*)-2-hydroxypropyl]amino}ethanone oxalate (8f)

To a solution of compound **4f** (1.30 g) in ethyl acetate (20 mL) and saturated aqueous sodium bicarbonate (25 mL) was added a solution of chloroacetyl chloride (0.75 mL) in ethyl acetate (5 mL) at 4 °C, and the reaction mixture was stirred at room temperature for 1 hour. The mixture was diluted with water, extracted with ethyl acetate, dried over magnesium sulfate and concentrated in vacuo to give 2-chloro-1-(1-cyclohexyl-5-fluoro-3,4-dihydroisoquinolin-2(1*H*)-yl)ethanone (971 mg 65%) as a colorless solid. FAB MS m/z 310 $[M+H]^+$. To a solution of compound 2-chloro-1-(1-cyclohexyl-5-fluoro-3,4-dihydroisoquinolin-2(1*H*)-yl)ethanone (290 mg) in acetonitrile (10 mL) was added potassium carbonate (736 mg), (2*R*)-1-amino-propanol (300 mg) and *N*,*N*,*N*-tributyl-1-butanaminium iodide (36 mg). The reaction mixture was stirred for 7 hours at 70 °C. The mixture was diluted with ethyl acetate and water, extracted with ethyl acetate, washed with brine, dried over magnesium sulfate and then concentrated in vacuo. The residue was purified by silica gel column chromatography, eluting with chloroform–methanol to give the desired product as a colorless oil (270 mg). The oil was dissolved in a solution of 2-propanol and ether, and oxalic acid (70 mg) was added to the solution. The precipitate was filtered off to obtain the title compound **8f** (290 mg, 68%) as a colorless solid. ^{1}H NMR (DMSO-d_6): This compound exists as a pair of rotamers at room temperature. δ 7.17–7.27 (1H, m), 6.98–7.14 (2H, m), 5.18 (major isomer 1H, d, J = 9.3 Hz), 4.36–4.46 (minor isomer 1H, m), 4.18 (major isomer 1H, dd, J = 2.5, 13.6 Hz), 3.91–4.09 (2H, m), 3.67–3.77 (major isomer 1H, m), 3.54–3.64 (major isomer 1H, m), 3.22–3.32 (minor

isomer 1H, m), 2.65–3.05 (4H, m), 1.48–1.79 (6H, m), 0.92–1.23 (8H, m); FAB MS *m*/*z*: 349 $[M+H]^+$.

5.1.15. 1-(1-Cyclohexyl-5-methoxy-3,4-dihydroisoquinolin-2(1*H*)-yl)-2-{[(2*R*)-2-hydroxypropyl]amino}ethanone oxalate (8g)

Compound **8g** was synthesized using a similar protocol to that for compound **8f**. Compound **8g** was obtained in 20% yield as a colorless solid. ^{1}H NMR (DMSO-d_6): This compound exists as a pair of rotamers at room temperature. δ 7.33–7.40 (1H, m), 7.14 (1H, t, J = 7.9 Hz), 6.84–6.91 (1H, m), 6.76 (1H, d, J = 7.7 Hz), 5.09 (major isomer 1H, d, J = 9.3 Hz), 4.32–4.41 (minor isomer 1H, m), 4.26–4.31 (minor isomer 1H, m), 4.17 (1H, d, J = 16.1 Hz), 3.89–4.08 (3H, m), 3.51–3.71 (2H, m), 3.18–3.28 (minor isomer 1H, m), 3.78 (3H, s), 2.85–2.98 (1H, m), 2.65–2.81 (2H, m), 1.50–1.79 (6H, m), 0.91–1.22 (8H, m); FAB MS *m*/*z*: 361 $[M+H]^+$.

5.1.16. 1-(1-Cyclohexyl-6-fluoro-3,4-dihydroisoquinolin-2(1*H*)-yl)-2-{[(2*R*)-2-hydroxypropyl]amino}ethanone oxalate (8h)

Compound **8h** was synthesized using a similar protocol to that for compound **8f**. Compound **8h** was obtained in 68% yield as a colorless solid. ^{1}H NMR (DMSO-d_6): This compound exists as a pair of rotamers at room temperature. δ 7.16–7.25 (1H, m), 6.96–7.13 (2H, m), 5.12 (major isomer 1H, d, J = 9.4 Hz), 4.31–4.40 (minor isomer 1H, m), 4.10–4.26 (1H, m), 3.90–4.07 (2H, m), 3.51–3.69 (major isomer 2H, m), 3.26–3.37 (minor isomer 1H, m), 2.69–3.06 (4H, m), 1.42–1.79 (6H, m), 0.90–1.23 (8H, m); FAB MS *m*/*z*: 349 $[M+H]^+$.

5.1.17. 1-(1-Cyclohexyl-6-methyl-3,4-dihydroisoquinolin-2(1*H*)-yl)-2-{[(2*R*)-2-hydroxypropyl]amino}ethanone oxalate (8i)

Compound **8i** was synthesized using a similar protocol to that for compound **8f**. Compound **8i** was obtained in 94% yield as a colorless solid. ^{1}H NMR (DMSO-d_6): This compound exists as a pair of rotamers at room temperature. δ 6.94–7.06 (3H, m), 5.06 (major isomer 1H, d, J = 9.3 Hz), 4.09–4.31 (1H, m), 3.90–4.06 (2H, m), 3.49–3.70 (major isomer 2H, m), 3.26–3.40 (minor isomer 1H, m), 2.68–3.00 (4H, m), 2.26 (3H, s), 1.47–1.81 (6H, m), 0.92–1.23 (8H, m); FAB MS *m*/*z*: 345 $[M+H]^+$.

5.1.18. 1-(1-Cyclohexyl-6-methoxy-3,4-dihydroisoquinolin-2(1*H*)-yl)-2-{[(2*R*)-2-hydroxypropyl]amino}ethanone oxalate (8j)

Compound **8j** was synthesized using a similar protocol to that for compound **8f**. Compound **8j** was obtained in 68% yield as a colorless solid. ^{1}H NMR (DMSO-d_6): This compound exists as a pair of rotamers at room temperature. δ 7.01–7.09 (1H, m), 6.77–6.81 (1H, m), 6.70–6.76 (1H, m), 5.05 (major isomer 1H, d, J = 9.3 Hz), 4.27–4.33 (minor isomer 1H, m), 4.15–4.24 (minor isomer 1H, m), 3.94 (minor isomer 1H, d, J = 7.0 Hz), 3.73–3.92 (2H, m), 3.72 (3H, s), 3.52–3.66 (2H, m), 3.22–3.30 (minor isomer 1H, m), 2.57–2.98 (4H, m), 1.47–1.75 (6H, m), 0.95–1.17 (8H, m); FAB MS *m*/*z*: 361 $[M+H]^+$.

5.1.19. 1-Cyclohexyl-2-{*N*-[(2*R*)-2-hydroxypropyl]glycyl}-1,2,3,4-tetrahydroisoquinoline-6-carboxamide oxalate (8k)

Compound **8k** was synthesized using a similar protocol to that for compound **8f**. Compound **8k** was obtained in 32% yield as a colorless solid. ^{1}H NMR (DMSO-d_6): This compound exists as a pair of rotamers at room temperature. δ 7.92 (1H, br s), 7.73 (1H, br s), 7.64–7.71 (1H, m), 7.33 (1H, br s), 7.20–7.27 (1H, m), 5.17 (major isomer 1H, d, J = 9.2 Hz), 4.35–4.44 (minor isomer 1H, m), 4.20–4.31 (minor isomer 1H, m), 4.15 (major isomer 1H, d, J = 16.1 Hz), 3.89–4.07 (2H, m), 3.55–3.73 (major isomer 2H, m), 3.30–3.42 (1H, m), 2.84–3.07 (3H, m), 2.64–2.81 (1H, m), 1.44–1.79 (6H, m), 0.94–1.21 (8H, m); FAB MS *m*/*z*: 361 $[M+H]^+$.

5.1.20. 1-(1-Cyclohexyl-7-fluoro-3,4-dihydroisoquinolin-2(1*H*)-yl)-2-{[(2*R*)-2-hydroxypropyl]amino}ethanone oxalate (8l)

Compound **8l** was synthesized using a similar protocol to that for compound **8f**. Compound **8l** was obtained in 97% yield as a colorless solid. ^{1}H NMR (DMSO-d_6): This compound exists as a pair of rotamers at room temperature. δ 7.18–7.31 (1H, m), 6.99–7.13 (2H, m), 5.15 (major isomer 1H, d, J = 9.2 Hz), 4.33–4.41 (minor isomer 1H, m), 4.09–4.24 (1H, m), 3.90–4.08 (2H, m), 3.53–3.71 (major isomer 2H, m), 3.28–3.38 (minor isomer 1H, m), 2.69–3.00 (4H, m), 1.43–1.78 (6H, m), 0.94–1.25 (8H, m); FAB MS *m*/*z*: 349 $[M+H]^+$.

5.1.21. 1-(1-Cyclohexyl-7-methyl-3,4-dihydroisoquinolin-2(1*H*)-yl)-2-{[(2*R*)-2-hydroxypropyl]amino}ethanone oxalate (8m)

Compound **8m** was synthesized using a similar protocol to that for compound **8f**. Compound **8m** was obtained in 91% yield as a colorless solid. ^{1}H NMR (DMSO-d_6): This compound exists as a pair of rotamers at room temperature. δ 7.09 (1H, d, J = 7.8 Hz), 7.04 (1H, d, J = 7.7 Hz), 6.96 (1H, s), 5.05 (major isomer 1H, d, J = 9.3 Hz), 4.23–4.29 (minor isomer 1H, m), 4.10–4.21 (1H, m), 3.91–4.06 (2H, m), 3.60–3.69 (major isomer 1H, m), 3.49–3.59 (major isomer 1H, m), 3.28–3.37 (minor isomer 1H, m), 2.70–2.99 (4H, m), 2.28 (minor isomer 3H, s), 2.27 (major isomer 3H, s), 1.47–1.77 (6H, m), 0.94–1.22 (8H, m); FAB MS *m*/*z*: 345 $[M+H]^+$.

5.1.22. 1-(1-Cyclohexyl-7-methoxy-3,4-dihydroisoquinolin-2(1*H*)-yl)-2-{[(2*R*)-2-hydroxypropyl]amino}ethanone oxalate (8n)

Compound **8n** was synthesized using a similar protocol to that for compound **8f**. Compound **8n** was obtained in 64% yield as a colorless solid. ^{1}H NMR (DMSO-d_6): This compound exists as a pair of rotamers at room temperature. δ 7.06–7.15 (1H, m), 6.77–6.85 (1H, m), 6.71–6.76 (1H, m), 5.09 (major isomer 1H, d, J = 9.2 Hz), 4.27–4.35 (minor isomer 1H, m), 3.87–4.19 (2H, m), 3.73 (minor isomer 3H, s), 3.72 (major isomer 3H, s), 3.49–3.68 (2H, m), 3.28–3.37 (minor isomer 1H, m), 2.68–2.95 (4H, m), 1.48–1.77 (6H, m), 0.96–1.20 (8H, m); FAB MS *m*/*z*: 361 $[M+H]^+$.

5.1.23. 1-(1-Cyclohexyl-8-fluoro-3,4-dihydroisoquinolin-2(1*H*)-yl)-2-{[(2*R*)-2-hydroxypropyl]amino}ethanone oxalate (8o)

Compound **8o** was synthesized using a similar protocol to that for compound **8f**. Compound **8o** was obtained in 63% yield as a colorless solid. ^{1}H NMR (DMSO-d_6): This compound exists as a pair of rotamers at room temperature. δ 7.23–7.32 (1H, m), 7.02–7.15 (2H, m), 5.47 (major isomer 1H, d, J = 10.0 Hz), 4.51 (minor isomer 1H, d, J = 8.7 Hz), 3.91–4.22 (3H, m), 3.69–3.79 (major isomer 1H, m), 3.49–3.60 (major isomer 1H, m), 3.36–3.45 (minor isomer 1H, s), 2.86–3.14 (3H, m), 2.69–2.83 (1H, m), 1.52–1.83 (5H, m), 1.30–1.43 (1H, m), 0.97–1.24 (8H, m); ESI MS *m*/*z*: 349 $[M+H]^+$.

5.1.24. 1-(1-Cyclohexyl-8-methoxy-3,4-dihydroisoquinolin-2(1*H*)-yl)-2-{[(2*R*)-2-hydroxypropyl]amino}ethanone oxalate (8p)

Compound **8p** was synthesized using a similar protocol to that for compound **8f**. Compound **8p** was obtained in 59% yield as a colorless solid. ^{1}H NMR (DMSO-d_6): This compound exists as a pair of rotamers at room temperature. δ 7.15–7.24 (1H, m), 6.78–6.91 (2H, m), 5.61 (major isomer 1H, d, J = 10.0 Hz), 5.60 (minor isomer 1H, d, J = 9.8 Hz), 3.83–4.18 (3H, m), 3.80 (minor isomer 3H, s), 3.77 (major isomer 3H, s), 3.68–3.76 (1H, m), 3.37–3.48 (1H, m), 2.70–3.12 (4H, m), 1.51–1.77 (5H, m), 1.25–1.35 (1H, m), 0.96–1.21 (8H, m); FAB MS *m*/*z*: 361 $[M+H]^+$.

5.1.25. 2-{[(2*R*)-2-Hydroxypropyl]amino}-1-[(1*S*)-1-phenyl-3,4-dihydroisoquinolin-2(1*H*)-yl]ethanone oxalate ((1*S*)-8q)

Compound (1*S*)-**8q** was synthesized using a similar protocol to that for compound **8f**. Compound (1*S*)-**8q** was obtained in 45% yield as a colorless solid. ^{1}H NMR (DMSO-d_6): This compound exists as a pair of rotamers at room temperature. δ 7.15–7.40 (9H, m), 6.66 (major isomer 1H, s), 6.17 (minor isomer 1H, br s), 4.38 (minor isomer 1H, d, J = 16.1 Hz), 4.22 (major isomer 1H, d, J = 16.2 Hz), 3.89–4.16 (2H, m), 3.60–3.70 (1H, m), 3.47–3.58 (1H, m), 3.35–3.45 (1H, m), 2.93–3.06 (2H, m), 2.72–2.91 (2H, m), 1.04–1.14 (3H, m); FAB MS m/z: 325 $[M+H]^+$. Anal. Calcd for $C_{20}H_{24}N_2O_2{\cdot}C_2H_2O_4$: C, 63.76; H, 6.32; N, 6.76. Found: C, 63.69; H, 6.33; N, 6.71. $[\alpha]_D^{26}$ +115.2° (c = 0.1, MeOH).

5.1.26. 1-(8-Fluoro-1-phenyl-3,4-dihydroisoquinolin-2(1*H*)-yl)-2-{[(2*R*)-2-hydroxypropyl]amino}ethanone oxalate (8r)

Compound **8r** was synthesized using a similar protocol to that for compound **8f**. Compound **8r** was obtained in 48% yield as a colorless solid. ^{1}H NMR (DMSO-d_6): This compound exists as a pair of rotamers at room temperature. δ 7.26–7.43 (4H, m), 7.07–7.23 (4H, m), 6.87 (major isomer 1H, br s), 6.17 (minor isomer 1H, d, J = 6.8 Hz), 4.42–4.51 (minor isomer 1H, m), 4.07–4.31 (2H, m), 3.93–4.04 (1H, m), 3.63–3.73 (1H, m), 3.30–3.42 (1H, m), 2.74–3.15 (4H, m), 1.10 (major isomer 3H, d, J = 6.2 Hz), 1.04 (minor isomer 3H, d, J = 6.2 Hz).

5.1.27. 2-{[(2*R*)-2-Hydroxypropyl]amino}-1-(8-methyl-1-phenyl-3,4-dihydroisoquinolin-2(1*H*)-yl)ethanone oxalate (8s)

Compound **8s** was synthesized using a similar protocol to that for compound **8f**. Compound **8s** was obtained in 44% yield as a colorless solid. ^{1}H NMR (DMSO-d_6): This compound exists as a pair of rotamers at room temperature. δ 7.19–4.40 (4H, m), 7.01–7.17 (4H, m), 6.80 (major isomer 1H, br s), 5.96 (minor isomer 1H, br s), 4.41 (minor isomer 1H, br s), 3.92–4.22 (3H, m), 3.56–3.68 (1H, m), 3.28–3.39 (1H, m), 2.90–3.09 (2H, m), 2.70–2.89 (2H, m), 2.10 (minor isomer 3H, d, J = 5.1 Hz), 2.03 (major isomer 3H, d, J = 3.4 Hz), 1.11 (3H, d, J = 6.2 Hz); ESI MS m/z: 339 $[M+H]^+$.

5.1.28. 2-{[(2*R*)-2-Hydroxypropyl]amino}-1-[(1*S*)-8-methoxy-1-phenyl-3,4-dihydroisoquinolin-2(1*H*)-yl]ethanone oxalate ((1*S*)-8t)

Compound (1*S*)-**8t** was synthesized using a similar protocol to that for compound **8f**. Compound (1*S*)-**8t** was obtained in 85% yield as a colorless solid. ^{1}H NMR (DMSO-d_6): This compound exists as a pair of rotamers at room temperature. δ 7.21–7.36 (4H, m), 7.14 (minor isomer 2H, d, J = 7.2 Hz), 7.08 (major isomer 2H, d, J = 7.1 Hz), 6.91–6.98 (1H, m), 6.84–6.90 (2H, m), 6.06 (minor isomer 1H, br s), 4.03–4.34 (2H, m), 3.93–4.03 (1H, m), 3.72 (minor isomer 3H, s), 3.71 (major isomer 3H, s), 3.53–3.63 (1H, m), 3.32–3.43 (1H, m), 2.91–3.05 (2H, m), 2.69–2.84 (2H, m), 1.07–1.13 (3H, m), 1.04 (1H, d, J = 6.2 Hz); FAB MS m/z: 355 $[M+H]^+$. Anal. Calcd for $C_{21}H_{26}N_2O_3{\cdot}C_2H_2O_4$: C, 62.15; H, 6.35; N, 6.30. Found: C, 61.92; H, 6.39; N, 6.22. $[\alpha]_D^{26}$ +97.8° (c = 0.1, MeOH).

5.1.29. 2-{[(2*R*)-2-Hydroxypropyl]amino}-1-[(1*R*)-8-methoxy-1-phenyl-3,4-dihydroisoquinolin-2(1*H*)-yl]ethanone fumarate ((1*R*)-8t)

Compound (1*R*)-**8t** was synthesized using a similar protocol to that for compound **8f**. Compound (1*R*)-**8t** was obtained in 41% yield as a colorless solid. ^{1}H NMR (DMSO-d_6): This compound exists as a pair of rotamers at room temperature. δ 7.19–7.34 (4H, m), 7.13 (minor isomer 2H, d, J = 7.2 Hz), 7.06 (major isomer 2H, d, J = 7.3 Hz), 6.82–6.97 (3H, m), 6.52 (fumaric acid 2H, s), 6.17 (minor isomer 1H, br s), 3.75–3.97 (3H, m), 3.73 (minor isomer 3H, s), 3.70 (major isomer 3H, s), 3.58–3.66 (1H, m), 3.29–3.49 (1H, m), 2.90–3.02 (1H, m), 2.61–2.78 (3H, m), 1.01–1.10 (3H, m); FAB MS m/z: 355 $[M+H]^+$. Anal. Calcd for $C_{21}H_{26}N_2O_3{\cdot}C_4H_4O_4$: C, 63.82; H, 6.43; N, 5.95. Found: C, 63.64; H, 6.42; N, 5.88. $[\alpha]_D^{26}$ −153.2° (c = 0.1, MeOH).

5.2. VCD analysis of (1*S*)-5-bromo-8-methoxy-1-phenyl-1,2,3,4-tetrahydroisoquinoline (1*S*)-22

An absolute configuration of compound (1*S*)-22 was assigned using vibrational dichroism (VCD) spectra.[7] See Supporting information.

5.3. Docking study of potent CYP2D6 inhibitor (1*S*)-8q

For docking simulation, the crystal structure of human cytochrome CYP2D6 in complex with 10-{2-[(2*R*)-1-methylpiperidin-2-yl]ethyl}-2-(methylsulfanyl)-10*H*-phenothiazine (RTZ, represented by residue name in the Protein Data Bank record 3TBG) was processed using the Protein Preparation Wizard of Maestro 9.7 (Schrodinger, Inc., New York, 2014) with default parameters. As the crystal structure contains four CYP2D6 molecules, we first removed discarded molecules for simulation and only one set of receptor, ligands and waters belonging to chain A were kept. The hydrogens were then added to them and energetically optimized using Prime. All docking processes were performed using Glide on Maestro 9.7. Given that the molecular size and pharmacophore positioning of RTZ are similar to that of (1*S*)-**8q**, grids defining the binding site were generated around one of two RTZ molecules observed in the crystal structure (RTZ1 in 3TBG).[10] All of the water molecules, including three blocking the route to HEME (HOH 614, 615 and 628 in 3TBG), were kept as part of the receptor during grid generation. This was intended to prevent (1*S*)-**8q** from positioning nearby heme. Docking calculation was performed with the default parameter of Glide SP protocol, without any intentional restraint, and the best *glidescore* mode was selected as the CYP2D6 binding model of (1*S*)-**8q**. To understand why (1*S*)-**8q** has potency to CYP2D6, putative interactions between them were visualized using MOE 2013 (Chemical Computing Group Inc., Quebec, 2014) and Scorpion (Desert Scientific Software, Australia, 2014).

5.4. Pharmacology

5.4.1. Inhibitory activity against N-type calcium channels was evaluated using an in vitro FLIPR assay in IMR-32 human neuroblastoma cells

IC_{50} values were determined in duplicate in one experiment. Details of experimental procedures were as previously described.[5a] For more advanced compounds, inhibitory activities were determined in several times of assays to obtain stable IC50 values with high confidence. These data will be published elsewhere.

5.4.2. Inhibitory activity against L-type calcium channels was evaluated using an in vitro FLIPR assay in IMR-32 human neuroblastoma cells

The inhibitory activity of (1*S*)-**8t** against L-type calcium channels was evaluated as previously described for the evaluation of inhibitory activity against N-type calcium channels[5a] using ω-conotoxin MVIIA instead of nitrendipine.

5.4.3. Evaluation of hERG inhibition using Rb Efflux assay

The inhibitory activity of (1*S*)-**8t** for hERG was evaluated using Rb efflux assay. Details of experimental procedures were as previously described.[5a]

5.4.4. Measurement of CYP inhibition

The inhibitory activities of test compounds for CYP1A2, 2C9, 2C19 and 2D6 were determined using a fluorescence-based assay. Details of experimental procedures have been described previously.[5a] For CYP3A4 inhibition assay, midazolam was used as a probe substrate to monitor changes in CYP3A4 activity during exposure to each test compound. Details of experimental procedures have also been described previously.[5a] Residual metabolic activities for reversible (Eq. 1) and time-dependent (Eq. 2) inhibition were calculated using the following equations, respectively:

$$\%\ \text{Residual Activity} = \text{Activity}_{\text{compound,0 min}}/\text{Activity}_{\text{vehicle,0 min}} \times 100 \quad (1)$$

$$\%\ \text{Residual Activity} = (\text{Activity}_{\text{compound,30 min}}/\text{Activity}_{\text{vehicle,30 min}})/(\text{Activity}_{\text{compound,0 min}}/\text{Activity}_{\text{vehicle,0 min}}) \times 100 \quad (2)$$

where $\text{Activity}_{\text{compound, 0 min}}$ denotes activity obtained in the presence of compound and without pre-incubation, $\text{Activity}_{\text{vehicle, 0 min}}$ denotes activity obtained in the absence of compound and without pre-incubation, $\text{Activity}_{\text{compound, 30 min}}$ denotes activity obtained in the presence of compound and with pre-incubation, and $\text{Activity}_{\text{vehicle, 30 min}}$ denotes activity obtained in the absence of compound and with pre-incubation.

5.4.5. Animal experiments

Male ddY mice or Sprague-Dawley rats (SLC, Hamamatsu, Japan) were used for in vivo experiments. Animals were group-housed and kept under a 12-hour light/dark cycle (lights on from 7:30 AM to 7:30 PM) with free access to food and water. All animal experimental procedures were approved by the Committee for Animal Experiments of Astellas Pharma Inc. and conformed to the International Guiding Principles for Biomedical Research Involving Animals (CIOMS) and Guidelines for Proper Conduct of Animal Experiments (Science Council of Japan, 2006). All efforts were made to minimize the number of animals used and their suffering.

We examined the antinociceptive effect of selected compounds in the mice formalin test previously published by Hunskaar et al.[14] with slight modifications. Details of the experimental procedures have been described previously.[5b] In addition, the efficacy of compound (1*S*)-**8t** in neuropathic pain was evaluated in the rat SNL model reported by Chung et al.[12] Evaluated compounds were suspended and diluted in 0.5% methylcellulose solution. The dose of drug is shown as the free form. Details of the experimental procedures have been described previously.[15]

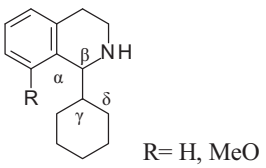

Figure 3. The dihedral angles of tetrahydroisoquinoline derivatives.

Acknowledgements

We wish to acknowledge Dr. Hiroshi Izumi (The National Institute of Advanced Industrial Science and Technology) for his help in the VCD analysis of (1*S*)-**22**. We thank Dr. Tatsuya Niimi for his valuable comments regarding the structural basis of drug binding to CYP2D6 enzyme. We also thank Drs. Kenichi Onda and Susumu Watanuki for their helpful advice and careful reading of the manuscript. In addition, we thank the staff of the Division of Analytical Science Laboratories for conducting the elemental analyses and spectral measurements.

Supplementary data

Supplementary data associated with this article can be found, in the online version, at http://dx.doi.org/10.1016/j.bmc.2015.05.053.

References and notes

1. (a) McGivern, J. G.; McDonough, S. I. *Curr. Drug Targets: CNS Neurol. Disord.* **2004**, *3*, 457; (b) McGivern, J. G. *Drug Discovery Today* **2006**, *11*, 245.
2. (a) Miljanich, G. P. *Curr. Med. Chem.* **2004**, *11*, 3029; (b) Schmidtkco, A.; Lötsch, J.; Freynhagen, R.; Geisslinger, G. *Lancet* **2010**, *375*, 1569.
3. (a) Yamamoto, T.; Takahara, A. *Curr. Top. Med. Chem.* **2009**, *9*, 377; (b) Barrow, J. C.; Duffy, J. L. *Annu. Rep. Med. Chem.* **2010**, *45*, 2; (c) Lee, M. S. *Prog. Med. Chem.* **2014**, *53*, 147.
4. (a) Beebe, X.; Yeung, C. M.; Darczak, D.; Shekhar, S.; Vortherms, T. A.; Miller, L.; Milicic, I.; Swensen, A. M.; Zhu, C. Z.; Banfor, P.; Wetter, J. M.; Marsh, K. C.; Jarvis, M. F.; Scott, V. E.; Schrimpf, M. R.; Lee, C.-H. *Bioorg. Med. Chem. Lett.* **2013**, *23*, 4857; (b) Shao, P. P. *ACS Med. Chem. Lett.* **2013**, *4*, 1064; (c) Winters, M. P.; Subashinghe, N.; Wall, M.; Beck, E.; Brandt, M. R.; Finley, M. F. A.; Liu, Y.; Lubin, M. L.; Neeper, M. P.; Qin, N.; Flores, C. M.; Sui, Z. *Bioorg. Med. Chem. Lett.* **2014**, *24*, 2053; (d) Winters, M. P.; Subashinghe, N.; Wall, M.; Beck, E.; Brandt, M. R.; Finley, M. F. A.; Liu, Y.; Lubin, M. L.; Neeper, M. P.; Qin, N.; Flores, C. M.; Sui, Z. *Bioorg. Med. Chem. Lett.* **2014**, *24*, 2057.
5. (a) Ogiyama, T.; Inoue, M.; Honda, S.; Yamada, H.; Watanabe, T.; Gotoh, T.; Kiso, T.; Koakutsu, A.; Kakimoto, S.; Shishikura, J. *Bioorg. Med. Chem* **2014**, *22*, 6899; (b) Ogiyama, T.; Yonezawa, K.; Inoue, M.; Watanabe, T.; Sugano, Y.; Gotoh, T.; Kiso, T.; Koakutsu, A.; Kakimoto, S.; Shishikura, J. *Bioorg. Med. Chem.* **2015**. accepted for publication.
6. (a) Zhou, S.-F.; Liu, J.-P.; Lai, X.-S. *Curr. Med. Chem.* **2009**, *16*, 2661; (b) Zhou, S.-F. *Curr. Pharm. Des.* **2008**, *14*, 990.
7. (a) Stephens, P. J.; Devlin, F. J.; Pan, J.-J. *Chirality* **2008**, *20*, 643; (b) Nafie, L. A.; Freedman, T. B. Vibrational Optical Activity Theory. In *Circular Dichroism: Principles and Applications*; Berova, N., Nakanishi, K., Woody, R. W., Eds., 2nd ed.; Wiley-VCH: New York, 2000; p 97.
8. (a) Brändén, G.; Sjögren, T.; Schnecke, V.; Xue, Y. *Drug Discovery Today* **2014**, *19*, 905; (b) Kumar, S.; Sharma, R.; Roychowdhury, A. *Curr. Med. Chem.* **2012**, *19*, 3605; (c) Stoll, F.; Göller, A.; Hillisch, A. *Drug Discovery Today* **2011**, *16*, 530; (d) Moroy, G.; Martiny, V. Y.; Vayer, P.; Villoutreix, B. O.; Miteva, M. A. *Drug Discovery Today* **2012**, *17*, 44; (e) Güner, O.; Bowen, J. P. *Curr. Top. Med. Chem.* **2013**, *13*, 1327.
9. (a) Bourdonnec, B.; Leister, L. *Curr. Med. Chem.* **2009**, *16*, 3093; (b) de Groot, M. J.; Wakenhut, F.; Whitlock, G.; Hyland, R. *Drug Discovery Today* **2009**, *14*, 964.
10. The crystal structure of human cytochrome CYP2D6 in complex with RTZ was registered by Wang et al. and available in RCSB protein data bank as PDB ID of 3TBG (http://www.rcsb.org/pdb/home/home.do).
11. Conformational analyses of 8-methoxytetrahydroisoquinoline and tetrahydroisoquinoline were conducted with Conformation Import module in MOE with MMFF94x force field. Potential energy of each conformation was calculated using PM6 method implemented in MOPAC 2012. The energetically lowest conformation was selected as the most stable one of 8-methoxytetrahydroisoquinoline and tetrahydroisoquinoline. The dihedral angles between tetrahydroisoquinoline and the 1-phenyl group were measured in MOE 2013 (Chemical Computing Group Inc., Quebec, 2014). The dihedral angle is represented by the angles between the plane defined by (Cα–Cβ–Cγ) and the plane (Cβ–Cγ–Cδ). Each carbon atom (α, β, γ, and δ) was assigned as depicted in Figure 3.
12. Kim, S. H.; Chung, J. M. *Pain* **1992**, *50*, 355.
13. Li, C.; Xiao, J. *J. Am. Chem. Soc.* **2008**, *130*, 13208.
14. Hunskaar, S.; Fasmer, O. B.; Hole, K. *J. Neurosci. Meth.* **1985**, *14*, 69.
15. Watabiki, T.; Kiso, T.; Kuramochi, T.; Yonezawa, K.; Tsuji, N.; Kohara, A.; Kakimito, S.; Aoki, T.; Matsuoka, N. *J. Pharmacol. Exp. Ther.* **2011**, *336*, 743.